European Society of Computational Methods in Sciences and Engineering (ESCMSE)

Journal of Numerical Analysis, Industrial and Applied Mathematics (JNAIAM)
vol. 19, no. 1-2, 2026, pp. 77-84
ISSN 1790–8140

Performance Evaluation of a Bi-Fluid Solar Collector Using Various Hybrid Nanofluids

M.M. Hasan[a, b] and K. Hriczó[a, 1]

[a)]Department of Analysis,
Faculty of Mechanical Engineering and Informatics,
University of Miskolc,
3515 Miskolc, Hungary

[b)]Department of Mechanical Power Techniques,
Basra Technological Technical Institute,
Southern Technical University,
Basra, Iraq

Received 7 August, 2025; accepted in revised form 31 October, 2025

Abstract: This study evaluates the thermal performance of a dual-purpose solar collector using various hybrid nanofluids at different liquid flow rates. The impact of a (50:50) mixture of 1% vol MWCNT-CuO/H_2O, 1% vol SWCNT-CuO/H_2O, and 0.1% vol ZrO-SiC/H_2O hybrid nanofluids, in comparison to water, has been analyzed numerically. Simulations were conducted using ANSYS Fluent CFD software, and the results were verified against experimental data from existing literature. The findings indicate that the hybrid nanofluids significantly improved liquid outlet temperatures compared to conventional water. Specifically, the use of SWCNT-CuO/H_2O enhanced the exit liquid temperature and heat gain by 11.5% and 38%, respectively. Consequently, this enhancement can improve the thermal efficiency of the solar collector, underscoring the potential of hybrid nanofluids to enhance the performance of dual-purpose solar systems, making them effective alternatives to water as heat transfer fluids.

Keywords: Bi-fluid collector, CFD simulation, hybrid nanofluids, thermal performance,

Mathematics Subject Classification: 80M12

PACS: 44.90.+c

1. Introduction

Enhancing the thermal performance of solar thermal systems is a crucial point for researchers. It can be achieved by developing heat transfer fluids, which can improve the heat transfer abilities and thus provide an increased of heat gain and thus increase the overall efficiency [1]. Conventional fluids, such as water, glycols, and their mixtures, often have low thermal conductivity and limited heat transfer abilities, which restrict their effectiveness in solar thermal collectors [2]. To address this issue, nano particles are added to formulate Mono Nanofluids (MNFs), which are characterized by their superior thermophysical properties, including thermal conductivity, making these fluids valuable for a range of applications [3]. In a recent development, researchers combined two different nanoparticles in a base liquid to formulate a new brand known as Hybrid Nanofluids (HNFs), which have superior thermophysical, optical, rheological, and morphological properties [4].

Several studies indicate that HNFs offer higher thermal performance over MNFs and other conventional liquids when they are used in Flat Plate Solar Collectors (FPSCs). Al-Shibli and Hussein [5] reviewed the utilization of HNFs to improve the thermal efficacy of FPSCs. Their review examined the methods for preparing HNFs, techniques for ensuring their stability, their thermophysical properties, and the challenges associated with them. They highlighted how HNFs can improve the performance of solar

[1] Corresponding author. E-mail: krisztian.hriczo@uni-miskolc.hu.

applications compared to other liquids. The authors concluded that water is the most effective base liquid, that a two-step preparation method provides greater stability, and that HNFs outperform MNFs. Elshazly et al. [6] studied the thermal efficiency of FPSC using Multi-Walled Carbon Nanotubes (MWCNTs) , aluminum oxide (Al2O3), and a hybrid (50:50%) of both under controlled conditions. The experiments focused on varying parameters such as solar radiation, nanoparticle volume proportion, and flow rates, testing four concentrations at three flow rates. The hybrid nanofluid boosted efficiency by 26%, 29%, and 18% at flow rates of 1.5 L/m, 2.5 L/m, and 3.3 L/m, respectively. MWCNTs offered the highest efficiency, particularly at 0.05 wt% and a flow of 3.5 L/s, outperforming Al2O3 by about 20%. The study recommends a hybrid approach, using 50% MWCNTs and Al2O3 for enhanced efficiency. Singh et al. [7] tested HNFs with copper (Cu)-MWCNTs and distilled water both experimentally and through CFD simulation. The study conducted on FPSC with variable inclination angles and various flowrates and concentrations. The results obtained depicted that the improvement in thermal efficiency was up to 26% at lower flow rates.

Verma et al. [8] experimentally assessed various nanofluids including CuO-MWCNT and MgO-MWCNT fluids against water. A variety of volume concentrations and mas flow rates have been tested, showing that MWCNTs/ water nanofluid outperform others, making FPSCs more efficient and compact. Furthermore, MgO-MWCNT nanofluid achieved energy and exergy efficiencies of 71.56% and 70.55%, respectively. Alsarraf et al. [9] conducted a numerical modeling study to investigate the performance of MgO-MWCNT/Therminol VP-1 in FPSC featuring a spiral-shaped tube under the influence of a magnetic field. Various parameters were examined during their research, including Reynolds number, volume fractions, spiral pitch ratio, and Hartmann number. The use of a spiral tube combined with HNFs and a magnetic field enormously enhanced the performance of FPSC, reporting in a peak exergy efficiency improvement of 36.14%, particularly at higher Reynolds numbers and volume fractions. Ahmed et al. [10] explores the enhancement of FPSC performance using a water-based HNF composed of hexagonal boron nitride (hBN) and chemically functionalized carbon nanotubes (CF-CNTs). The experiments were conducted under a variety of weight concentrations and liquid flow rates, focusing on thermophysical properties, rheological behavior, and FPSC thermal efficiency. The findings show up to 87% collector efficiency at 0.1 wt.% and 4 L/min, a 24.8% improvement over distilled water, with stable, Newtonian fluid behavior suitable for solar applications. They found that a water-based HNF with hBN/CF-CNTs yielded a 34.36% increase in thermal conductivity at 60 °C.

Lee et al. [11] experimentally investigated the performance of water, MWCNTs, and Fe3O4 nanofluids in FPSC with vacuum tubes. Different mixing ratios of nanoparticles were used during the experiments to compare performance of solar collectors. The findings indicated that the application of 0.005 vol.% MWCNT/0.01 vol.% Fe3O4 achieved the highest efficiency of 80.3%, marking a 28.1% improvement over water. In the vacuum tube collector, this binary nanofluid reached an efficiency of 79.8%, representing a 45.4% enhancement compared to water. Additionally, increasing the mass flux of the nanofluid led to efficiency increases of 7.8% for the flat plate and 8.3% for the vacuum tube collectors. Green synthesizing carbon-based hybrid nanofluids were experimentally investigated by Alfellag et al. [12]. They focused on enhancing the thermal performance of FPSC using eco-friendly clove-treated carbon nanotubes/titanium dioxide (CT-MWCNTs/TiO_2) nanocomposites in a 60% to 40% ratio, dispersed in distilled water. The experiment assessed energy and exergy efficiency, as well as hydrothermal performance, under various weight concentrations, flow rates, heat flux intensities, and inlet temperatures. Results indicated a maximum energy efficiency improvement of 20.6% and exergy efficiency enhancement of 22.9% at 0.1 wt% and 1.2 L/min, alongside a 20.5% reduction in solar collector size.

A recent study by Ajeena et al. [13] investigated the use of a hybrid nanofluid made from ZrO2-SiC nanoparticles mixed with distilled water in a FPSC. The research evaluates the stability and thermo-physical properties of the nanofluid according to ASHRAE standards. Results showed that the FPSC achieved a maximum thermal efficiency of 75.21% with the nanofluid, marking a 31.64% improvement over pure distilled water. Exergy efficiency also increased by 28.31% at a volume fraction of 0.1% and a mass flow rate of 0.041 kg/s, though higher mass flow rates adversely affected exergy performance. The study underscores the potential of nanoparticles to enhance FPSC efficiency and emphasizes the limited existing literature on this specific hybrid nanofluid in renewable energy applications.

The aim of this study is to investigate the performance of a Dual-Purpose Solar Collector (DPSC) through numerical analysis, utilizing three different types of hybrid nanofluids (HNFs): 1% vol MWCNT-CuO/H_2O, 1% vol SWCNT-CuO/H_2O, and 0.1% vol ZrO-SiC/H_2O. The novelty of this research lies in the application of HNFs, specifically the ZrO-SiC/H_2O nanofluid in DPSC, which, to the best of the author's knowledge, has not been previously explored. There has been no prior research on the use of HNFs in a DPSC, making the investigation of ZrO-SiC/H_2O particularly significant, as only one publication has examined this type of fluid concerning its impact on DPSC performance. This uniqueness inspires the author to further explore the potential of this nanofluid in DPSC applications.

2. Modeling of DPSC

In the current work, ANSYS Fluent simulation has been utilized to analyze the DPSC which has the same design as that created by Assari et al. [14]. It comprises a single glass cover and an absorbent plate, along with seven liquid tubes bonded in parallel at the lower section, which are attached to the absorbed by the absorber plate. Furthermore, there are seven V-corrugated air channels bonded at the upper section, which are fixed to the top of the absorber and linked to the back insulation from underneath (see Fig. 1).

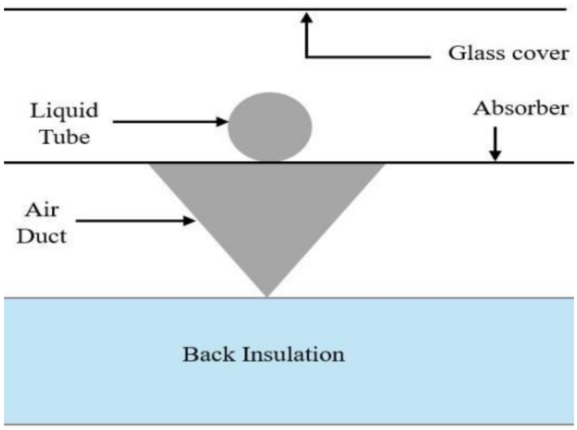

Figure 1: Schematic of the DPSC system studied.

The steady-state, three-dimensional fluid flow and conjugate heat transfer within the computational domain of the DPSC are governed by the continuous partial differential equations of conservation of mass, momentum, and energy. Treating the hybrid nanofluids as stable, homogeneous, single-phase Newtonian mixtures, the fluid flow is modeled using standard vector notation as follows:
Conservation of Mass (Continuity):

$$\nabla(\rho V) = 0 \tag{1}$$

Conservation of Momentum:

$$\nabla(\rho VV) = -\nabla \mathrm{p} + \nabla(\mu \nabla \mathrm{V}) \tag{2}$$

Conservation of Energy:

$$\nabla(\rho\, CpVT) = \nabla(\mathrm{k}\nabla \mathrm{T}) \tag{3}$$

where V represents the velocity vector, p is static pressure, T is temperature, and ρ, μ, Cp and k denote the effective density, dynamic viscosity, specific heat capacity, and thermal conductivity of the heat transfer fluid, respectively.

The three-dimensional shape of the DPSC is created utilizing the ANSYS Design Modeler, focusing on half of an air duct and water tube to streamline calculations. By incorporating symmetrical planes, a semi-circular design with a symmetric wall was developed, reducing mesh elements needed and enhancing mesh quality while decreasing analysis time. The conformal mesh, as shown in Fig. 2, consists of tetrahedron elements with structured prism layers and a growth rate of 1.01. Named selections in Fluent meshing define the boundary conditions, with symmetry boundaries minimizing the computational domain by leveraging mirror symmetry.

Furthermore, at the solid-fluid interfaces a conjugate heat transfer (coupled) boundary condition was enforced. This guarantees continuity of both temperature and heat flux across the physical boundary interfaces.

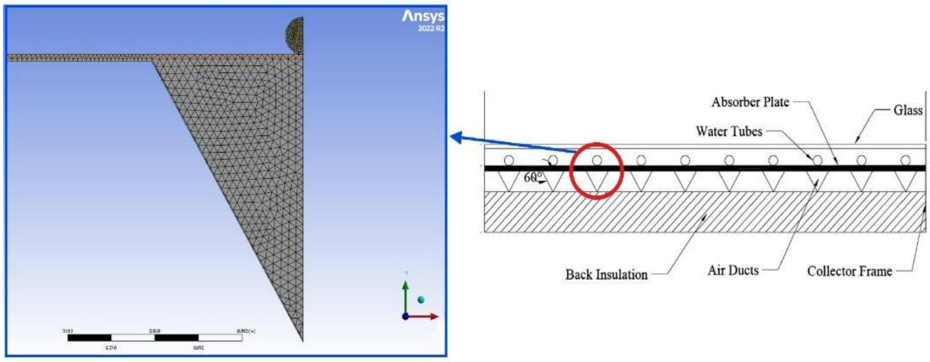

Figure 2: The cross-sectional view of the DPSC and its corresponding mesh configuration.

The mesh quality is verified through a grid-independence test, ensuring results depend on the model rather than mesh size. The number of mesh elements increased from 595,182 to 1,334,844, showing no significant temperature changes beyond 1,308,692 elements (Fig. 3). The average mesh quality metrics—skewness and orthogonal quality—are 0.78983, 0.12956, and 0.87791, considered suitable for reliable computations.

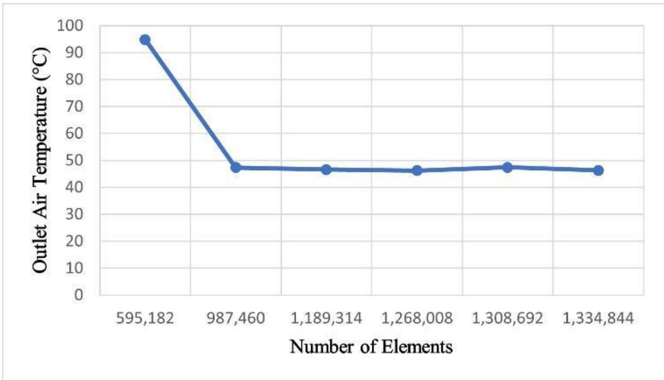

Figure 3: Mesh independence test.

The Grid Convergence Index (GCI) was calculated using three representative meshes: Coarse ($N3 = 595\,182$), Medium ($N2 = 987\,460$), and Fine ($N1 = 1\,308\,692$). Using the outlet air temperature as the target parameter (f), the grid refinement ratio (r) and the relative error (ε) were computed using Equations (4) and (5), respectively:

$$\mathrm{r} = \left(N_{fine}/N_{coarse}\right)^{(1/3)}, \tag{4}$$

$$\varepsilon = |(f_1 - f_2)/f_2|. \tag{5}$$

Thus

$$GCI = (F_s\varepsilon)/(r^p - 1). \tag{6}$$

where (F_s) is a safety factor, typically 1.25 for three grids, and the superscript (p) is the formal order of accuracy, typically 2, matching the second-order upwind discretization schemes applied in the solver. The evaluated fine-grid convergence index (GCI_{12}) dropped to a strict value of 0.18%, mathematically demonstrating that the solution is clear of significant spatial discretization error (see *Table 1*).

To maintain strict numerical error bounds during runtime, the finite volume algebraic linear solvers were monitored until normalized residuals dropped below tightly enforced limits. The numerical convergence thresholds were set to less than 10^{-5} for the continuity and momentum equations, and less than 10^{-6} for the energy equation.

To bridge the continuous physical model governed by Equations (1)–(3) with a computationally tractable solution, the computational domain of the DPSC is solved by leveraging a rigorous Finite Volume

Method (FVM) framework. The continuous partial differential equations are integrated over each control volume, converting the transport equations into a system of non-linear algebraic equations.

Table 1: Grid Convergence Index (GCI) metrics

Mesh Level	**Elements (N)**	**Outlet Air Temp (Tout, ∘C)**	**Relative Error (ϵ)**	**GCI (%)**
3 (Coarse)	595,182	95.0	—	—
2 (Medium)	987,460	47.5	50.00%	12.80%
1 (Fine)	1,308,692	47.2	0.63%	0.18%

To resolve the intrinsic numerical challenges of pressure-velocity coupling in the momentum equations, the Semi-Implicit Method for Pressure-Linked Equations (SIMPLE) algorithm is implemented. Spatial discretization relies on a second-order upwind scheme for the convective terms of momentum and energy equations. This choice mitigates numerical diffusion errors typical of first-order approximations while maintaining numerical stability, ensuring that transport properties across cell faces are interpolated with a formal second-order accuracy.

The current simulation study involves utilizing HNFs: MWCNT-CuO and SWCNT-CuO, each at 1% concentration (50:50), and ZrO_2-SiC at 0.1% concentration (50:50) in the DPSC as HTFs alongside water. *Table 2* shows the properties of the HNFs utilized in the current simulation, which serve as inputs for the ANSYS setup.

Table 2: Thermophysical properties of the various HNFs used in the simulation.

Physical properties	**ZrO_2- SiC** [13]	**MWCNT- CuO** [15]	**SWCNT- CuO** [15]
ρ **(kg/m3)**	1002.55400	1003.13200	1013.12900
K **(W/(m K))**	0.78500	0.61640	0.61640
C_p **(J/(kg K))**	4163.20000	4127.9900	4085.58000
μ **(mPa·s)**	0.00165	0.00105	0.00105

3. Results and discussion

During the simulation, the fluid flow regime is assumed to be laminar and four distinct cases have been created and analyzed, each case employs unique liquids. Additionally, the solar radiation kept at 900 W/m², with air flow rate is maintained at 0.1 kg/s, while the liquid flow rate varies from 0.02 kg/s to 0.1 kg/s, keeping the inlet temperature of air and liquid fixed at 45ºC and 40ºC, respectively. Therefore, in total, twenty simulation processes are conducted throughout this study, and the results are discussed in this section. To validate the current simulation, the outlet air temperatures obtained from the numerical findings were compared with experimental results obtained from [14] as shown in Fig. 4, revealing relative errors ranging from 1.044% to 0.085%.

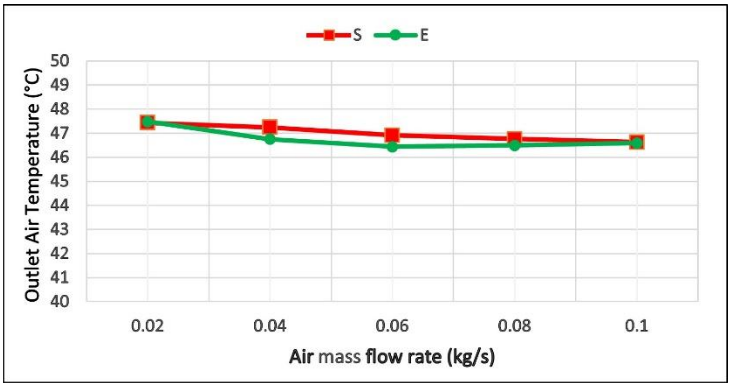

Figure 4: Experimental validation of numerical results (S= Simulation, E= Experimental).

The exit liquid temperatures and total heat gain of the DPSC with varying liquid mass flow are illustrated in Fig. 5a and b. Increasing the mass flow rate reduces the outlet temperature due to less time for heat transfer. Notably, the highest outlet temperature of 50.38 °C occurs at 0.02 kg/s with SWCNT-CuO/H_2O, compared to about 45 °C for other liquids. This results in a temperature drop of 6.5 °C for SWCNT-CuO/H_2O, while other liquids show only 2.8 °C.

The heat gain of the DPSC, shown in Fig. 5b, increases with higher liquid mass flow rates due to improved convective heat transfer. SWCNT-CuO/H_2O achieved the highest heat gain of 1587.9 W, followed by ZrO-SiC/H_2O at 1182 W, MWCNT-CuO/H_2O at 1166.3 W, and water at 1152 W. SWCNT-CuO/H_2O demonstrated a 37.8% increase in heat gain compared to water.

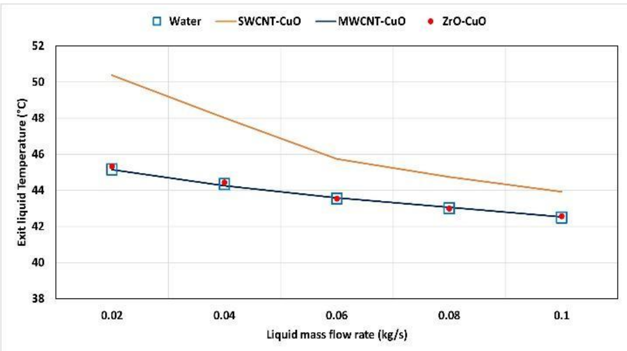

a)

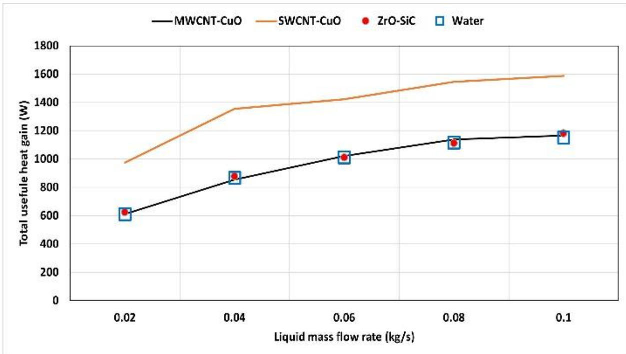

b)

Figure 5: The variation of a) exit liquid temperature and b) total heat gain of the DPSC with liquid mass flow rate.

4. Summary and future work

In the current investigation, ANSYS Fluent was used to evaluate the impact of using HNFs in DPSC. It was concluded that SWCNT-CuO/H_2O liquid significantly improves the overall thermal performance of the DPSC when compared to MWCNT-CuO/H_2O and ZrO-SiC/H_2O liquids. The improvement in exit liquid temperature and total heat gain are recorded at 11.5% and 38%, respectively. This indicates that this particular HNF can be effectively applied in DPSC applications.

Future recommended work includes conducting CFD simulations and exploring a wider variety of heat transfer fluids (HTFs), including nanofluids and other innovative mixtures. These investigations may provide valuable insights into optimizing the performance of the DPSC.

Furthermore, future studies could assess the maximum potential savings in coal, gas, and electricity from using coal-fired, gas, and electric boilers with different liquids in the collector, contributing to an environmental assessment.

Acknowledgments

The author wishes to thank the anonymous referees for their careful reading of the manuscript and their fruitful comments and suggestions.

References

[1] M. AbdEl-Rady Abu-Zeid et al., Performance enhancement of flat-plate and parabolic trough solar collector using nanofluid for water heating application, *Results in Engineering*, vol. 21, p. 101673, Mar. 2024, doi: 10.1016/J.RINENG.2023.101673.

[2] P. Raj and S. Subudhi, A review of studies using nanofluids in flat-plate and direct absorption solar collectors, *Renewable and Sustainable Energy Reviews*, vol. 84, pp. 54–74, Mar. 2018, doi: 10.1016/J.RSER.2017.10.012.

[3] A. O. Borode, N. A. Ahmed, P. A. Olubambi, M. Sharifpur, and J. P. Meyer, Investigation of the Thermal Conductivity, Viscosity, and Thermal Performance of Graphene Nanoplatelet-Alumina Hybrid Nanofluid in a Differentially Heated Cavity, *Front Energy Res*, vol. 9, p. 737915, Aug. 2021, doi: 10.3389/FENRG.2021.737915/BIBTEX.

[4] O. Al-Oran and F. Lezsovits, Thermal performance of inserting hybrid nanofluid in parabolic trough collector, *Pollack Periodica*, vol. 16, no. 3, pp. 88–93, Apr. 2021, doi: 10.1556/606.2021.00318.

[5] K. A. Al-Shibli and A. K. Hussein, Enhancement the Performance of FPSC by Utilizing Hybrid Nanofluids - An Extended Review, *International Journal of Heat and Technology*, vol. 42, no. 6, pp. 1901–1910, Dec. 2024, doi: 10.18280/IJHT.420607.

[6] E. Elshazly, A. A. Abdel-Rehim, and I. El-Mahallawi, 4E study of experimental thermal performance enhancement of flat plate solar collectors using MWCNT, Al2O3, and hybrid MWCNT/ Al2O3 nanofluids, *Results in Engineering*, vol. 16, p. 100723, Dec. 2022, doi: 10.1016/J.RINENG.2022.100723.

[7] S. Singh, K. Mausam, S. K. Ghosh, and A. K. Tiwari, An experimental and numerical approach for thermal performance investigation of solar flat plate collector, *Environmental Science and Pollution Research*, vol. 30, no. 40, pp. 92859–92879, Aug. 2023, doi: 10.1007/S11356-023-28843-9/FIGURES/18.

[8] S. K. Verma, A. K. Tiwari, and D. S. Chauhan, Experimental evaluation of flat plate solar collector using nanofluids, *Energy Convers Manag*, vol. 134, pp. 103–115, Jan. 2017, doi: 10.1016/j.enconman.2016.12.037.

[9] J. Alsarraf, A. A. Alnaqi, and A. A. A. A. Al-Rashed, Simulation of two-phase hybrid nanofluid flow in a flat plate solar collector equipped with spiral absorber tube under the influence of magnetic field: Hydraulic-thermal, energy, and exergy analysis, *J Magn Magn Mater*, vol. 585, Nov. 2023, doi: 10.1016/j.jmmm.2023.171120.

[10] M. Ahmed, M. M. Meteab, Q. O. Salih, H. A. Mohammed, and O. A. Alawi, Experimental Investigation on the Thermophysical and Rheological Behavior of Aqueous Dual Hybrid Nanofluid in Flat Plate Solar Collectors, *Energies 2020*, Vol. 15, Page 8541, vol. 15, no. 22, p. 8541, Nov. 2022, doi: 10.3390/EN15228541.

[11] M. Lee, Y. Shin, and H. Cho, Performance Evaluation of Flat Plate and Vacuum Tube Solar Collectors by Applying a MWCNT/Fe3O4 Binary Nanofluid, *Energies 2020*, Vol. 13, Page 1715, vol. 13, no. 7, p. 1715, Apr. 2020, doi: 10.3390/EN13071715.

[12] M. A. Alfellag et al., Green synthesized clove-treated carbon nanotubes/titanium dioxide hybrid nanofluids for enhancing flat-plate solar collector performance, *Appl Therm Eng*, vol. 246, p. 122982, Jun. 2024, doi: 10.1016/J.APPLTHERMALENG.2024.122982.

[13] A. M. Ajeena, I. Farkas, and P. Víg, Performance enhancement of flat plate solar collector using ZrO2-SiC/DW hybrid nanofluid: A comprehensive experimental study, *Energy Conversion and Management: X*, vol. 20, p. 100458, Oct. 2023, doi: 10.1016/J.ECMX.2023.100458.

[14] M. R. Assari, H. Basirat Tabrizi, and I. Jafari, Experimental and theoretical investigation of dual purpose solar collector, *Solar Energy*, vol. 85, no. 3, pp. 601–608, 2011, doi: 10.1016/j.solener.2011.01.006.

[15] H. Nabi, M. Pourfallah, M. Gholinia, and O. Jahanian, Increasing heat transfer in flat plate solar collectors using various forms of turbulence-inducing elements and CNTs-CuO hybrid nanofluids, *Case Studies in Thermal Engineering*, vol. 33, May 2022, doi: 10.1016/j.csite.2022.101909.